



## OPEN Irisin suppressed the progression of TBI via modulating AMPK/MerTK/autophagy and SYK/ROS/inflammatory signaling

Kuo Zhang<sup>1,2</sup>, Yihui Du<sup>2</sup>, Sihui Yang<sup>2</sup> & Guozhu Sun<sup>1,3</sup>✉

Irisin is a hormone-like peptide secreted by muscle tissues and generated by hydrolysis of type III fibronectin domain-containing protein 5 by proteolytic hydrolases. Whether Irisin has a potential protective role in traumatic brain injury (TBI). In this study, we will investigate the relevant research progress of Irisin's protective role in traumatic brain injury (TBI) in recent years in terms of attenuating oxidative stress, inhibiting pyroptosis, suppressing inflammatory response, and improving autophagy, with the aim of providing valuable references for the diagnosis and treatment of traumatic brain injury (TBI). Utilize bioinformatics analysis to study the interactions between genes in TBI (Traumatic Brain Injury). Construct a TBI mouse model to observe the effects of Irisin on TBI. The Morris water maze test is used to assess the learning and spatial memory abilities of mice, TUNEL fluorescence is used to detect cell apoptosis, Nissl staining is employed to observe the survival of hippocampal neurons in mice, and HE staining is used to observe the extent of brain injury in mice. Western blot is used to detect protein expression in both in vivo and in vitro experiments. Q-PCR is employed to detect the levels of proteins related to autophagy/pyroptosis/inflammation. Irisin promotes MerTK overexpression by enhancing AMPK activation. Irisin can increase the expression of LC3I and Beclin-1 proteins, indicating the promotion of autophagic response. Additionally, Irisin reduces ROS levels and decreases SYK expression, thereby inhibiting the inflammatory response. Irisin improves the learning and spatial memory abilities of TBI mice and reduces cell apoptosis, as well as decreases hippocampal neuron death. HE staining shows that the brain injury in mice treated with Irisin is significantly alleviated. Irisin can enhance the expression of phosphorylated AMPK and phosphorylated MerTK proteins, promote autophagic response, and inhibit pyroptosis/inflammatory response. Correction experiments confirmed that after stimulation with an AMPK agonist, the expression of phosphorylated MerTK protein is significantly increased, autophagic response is enhanced, and pyroptosis/inflammatory response is weakened. When treated with a MerTK inhibitor during AMPK agonist stimulation, the autophagic response is weakened while pyroptosis/inflammatory response is enhanced. Irisin can inhibit the progression of traumatic brain injury by regulating AMPK/MerTK/autophagy and SYK/ROS/inflammatory signaling.

**Keywords** Irisin, Traumatic brain injury (TBI), AMPK/MerTK, SYK/ROS, Autophagy, Focal death

### Abbreviations

AICAR	5-Aminoimidazole-4-carboxamide ribonucleotide
AMPK	AMP-activated protein kinase
ASC	Apoptosis-associated Speck-like protein containing a CARD
Beclin-1	Autophagy-related protein
BAI-1	Brain-specific Angiogenesis Inhibitor 1
cGAMP	Cyclic GMP-AMP
Caspase-1/4	Cysteine-aspartic proteases
Dectin-1	C-type lectin receptor

<sup>1</sup>Department of Neurosurgery, The Second Hospital of Hebei Medical University, Shijiazhuang City 050000, Hebei Province, China. <sup>2</sup>Department of Neurosurgery, Hebei General Hospital, Shijiazhuang City 050000, Hebei Province, China. <sup>3</sup>Department of Neurosurgery, The Second Hospital of Hebei Medical University, 215 Heping West Road, Xinhua District, Shijiazhuang City 050000, Hebei Province, China. ✉email: Sungzh705@hebmu.edu.cn

DEGs	Differentially expressed genes
DAMPs	Damage-Associated Molecular Patterns
ELISA	Enzyme-linked immunosorbent assay
FcγR	Fc Gamma Receptor
GAPDH	Glyceraldehyde-3-phosphate dehydrogenase
GO	Gene Ontology
GSH	Glutathione
Gas6	Growth Arrest-Specific 6
GSDMD	Gasdermin D
HMGB1	High mobility group box 1
HE Staining	Hematoxylin and Eosin Staining
IL-1β	Interleukin-1 beta
KEGG	Kyoto Encyclopedia of Genes and Genomes
KLF4	Krüppel-like factor 4
LC3	Microtubule-associated protein 1 A/1B-light chain 3
limma	Linear Models for Microarray Data
MDA	Malondialdehyde
MerTK	MER proto-oncogene tyrosine kinase
NLRP3	NLR family pyrin domain containing 3
NOX4	NADPH oxidase 4
PGC-1α	Peroxisome proliferator-activated receptor gamma coactivator 1-alpha
qPCR	Quantitative polymerase chain reaction
RBC	Red blood cell
SOD	Superoxide dismutase
SYK	Spleen tyrosine kinase
TBI	Traumatic brain injury
TLR	Toll-like Receptor
TUNEL	Terminal deoxynucleotidyl transferase dUTP Nick-End Labeling
TNF-α	Tumor necrosis factor-alpha

Traumatic brain injury (TBI) is defined as a disorder of brain function or any other evidence of brain pathology caused by an external force<sup>1</sup>. TBI is a devastating condition that can lead to paralysis and related complications<sup>2</sup>. Initial traumatic injury is followed by a series of secondary events characterized by local ischemia, hemorrhage, inflammation, edema, and further tissue damage, leading to demyelination, axonal degeneration, and also cavitation at the site of injury<sup>3,4</sup>. Statistically, TBI affects approximately 2.5 million people worldwide, with more than 130,000 new injuries reported annually. The treatment of TBI remains one of the greatest challenges for basic science and clinical researchers<sup>5</sup>. Although several therapies have been explored, they have shown limited efficacy.

Damage-associated molecular patterns (DAMPs) emerge after TBI stimulate local cells to release inflammatory mediators, such as cytokines and chemokines<sup>6</sup>, leading to tissue destruction, neurodegeneration, and autoimmune diseases<sup>7</sup>. In DAMPs, the nuclear transcription factor-κB (NF-κB) signaling pathway is a key signaling pathway that senses and integrates a large number of environmental and intracellular stimuli to integrate coordinated responses throughout the organism. During the initiation phase of inflammatory activation, Toll-like receptors (TLR)-induced NF-κB activates nucleotide-binding oligomerization of structural domain-like receptor protein 3 (NOD-like receptor protein 3 (NLRP3)) and interleukin-1β (IL-1β) genes, leading to the activation of the NOD-like receptor protein 3 (NLRP3) and IL-1β genes. Upregulation of NLRP3 and IL-1β transcription induces an inflammatory response in the body<sup>8–10</sup>. NLRs are cytoplasmic pattern recognition receptors (PRRs), consisting of a sensor molecule, an adapter protein, and an effector part, which play an important role in the inflammatory response<sup>11,12</sup>. NOD-like receptor family pyrin domain containing 3 (NLRP3) is a sensor of inflammatory vesicles<sup>13</sup>, the adapter protein is an apoptosis-associated speck-like protein containing a CARD (ASC)<sup>14</sup>, and caspase-1 is an effector protein that acts on inflammatory cytokines to cause cellular pyroptosis<sup>15</sup>. Pyroptosis, a new type of programmed cell death discovered in recent years, is characterized by the continuous swelling of cells until the cell membrane ruptures, leading to the release of cellular contents and the generation of a strong inflammatory response<sup>16</sup>.

Autophagy is a catabolic process whose formation and regulation are tightly controlled; it plays an important role in maintaining intracellular homeostasis by facilitating the recycling of lysosomal degradation of intracellular misfolded proteins and damaged organelles to maintain nutrient and energy homeostasis<sup>17</sup>.

There is growing evidence that Mer tyrosine kinase (MerTK) attenuates inflammatory responses. Phosphatidylserine (PtdSer) is an important phospholipid widely found in cell membranes. PtdSer is transferred from the inner membrane to the outer membrane layer, which is an early sign of apoptosis. This process helps phagocytes to recognize and remove apoptotic cells. PtdSer also plays an important role in the nervous system, participating in neuronal signaling and functional regulation of cell membranes<sup>18,19</sup>. In the present study, we investigated the role of MerTK in PtdSer activation in microglia and evaluated the contribution of Irisin to TBI.

Irisin, a muscle factor discovered in 2012, is thought to bridge the connection between muscle and other tissues in the body, acting on adipose tissue, skeletal muscle, liver, and pancreas<sup>20</sup>, and is an option for the prevention and treatment of metabolic disorders. In 2012, Spiegelman et al. first described the physiological role of Irisin in inducing thermogenic beige lipogenesis to control energy metabolism<sup>21</sup>. Since then, it has been shown to promote hepatic glycogen synthesis, inhibit hepatic gluconeogenesis, and maintain glucose homeostasis<sup>22,23</sup>.

Later, Irisin was found to function in the nervous system by improving cognition, learning, and memory<sup>24</sup>. In addition, Irisin maintains musculoskeletal homeostasis by binding to integrin  $\alpha V\beta 5$ <sup>25,26</sup>.

Ye et al. in their study demonstrated that Irisin may act on p38-mitogen-activated protein kinase (p38-MAPK)/peroxisome-proliferator-activated receptor gamma coactivator-1 alpha (PGC-1 $\alpha$ ) pathway to activate autophagy, setting the stage for the treatment of TBI using Irisin<sup>27</sup>. Other studies have shown that Irisin increases hepatic gluconeogenesis and reduces gluconeogenesis by driving the activation of PI3 K/AKT and adenosine monophosphate activated protein kinase (AMPK) in mouse and human primary hepatocytes, Hep G2 and DM mice<sup>28,29</sup>. It has been demonstrated that Irisin enhances autophagosome formation and autophagic flow levels and reduces apoptosis levels in insulinoma-1 (INS-1) cells cultured in vitro<sup>30</sup>. Currently, there is a debate on whether Irisin can regulate autophagy through the AMPK/MerTK pathway and inhibit the oxidative stress response as well as the pyroptosis/inflammatory response, thereby ameliorating the extent of TBI injury, to provide a theoretical basis for the treatment of TBI.

## Methods

### Raw letter analysis

The Gene Expression Omnibus database provided the dataset GSE2871, which is connected to traumatic brain injury (TBI). Eight control samples and seven TBI samples were included in the dataset GSE2871 at four and twenty-four hours following TBI, respectively. The limma software was used to determine the DEGs between the cortical samples from TBI and control.  $|\log_2 \text{Fold Change}| > 1$  and a p-value  $< 0.05$  were the thresholds. The ggplot2 software was used to visualise the analysis of variance findings. The ClusterProfiler software was used to conduct pathway enrichment studies for the Kyoto Encyclopaedia of Genes and Genomes (KEGG) and Gene Ontology (GO).

### Experimental animals and grouping

A total of 175 male C57BL/6 mice, weighing  $20 \pm 1$  g at 6 weeks of age, were acquired from Henan SKBS Life Technology Co. They were kept in a hygienic animal room with a 12:12 h light/dark cycle, a temperature of  $(24 \pm 2)^\circ\text{C}$ , and a relative humidity of 40–60%. The Hebei General Hospital Ethics Committee gave its approval to the planning and execution of the animal research. All experiments were performed in accordance with relevant guidelines and regulations. The study was carried out in compliance with the ARRIVE guidelines (<https://arriveguidelines.org>).

The mice were anaesthetised using 4.5% isoflurane, and the anaesthesia was maintained using 2% isoflurane gas at a flow rate of 0.2/min (mouse respiratory rate: 120 times/min, tidal volume: 1 ml/min) to eliminate the influence of cerebral blood flow on modelling. The head of the mice was fixed by ear bars while the incisors were stuck on the occlusal bars and placed prone on the stereotaxic apparatus. The head coat was removed with a razor blade and wiped with an alcohol cotton ball, followed by a longitudinal incision of about 1 cm along the median line to separate the periosteum. A 2.5-mm-diameter ring drill was used to cut the skull in a circular pattern 1 mm in front of the fontanel and 2 mm to the right of the coronal suture. When the skull was about to be cut apart, the circular bone piece was carefully lifted off with a sharp blade, and the dura was exposed by removing the bone piece with forceps, making sure that the dura was not injured during the above operation. A 2-mm-diameter impingement needle was then selected and mounted so that it contacted the surface of the dura mater without generating pressure. The parameters of the controlled cortical impact device were set to 3.5 m/s, 1.5 mm depth of impact, and 150 ms duration of impact, and the firing pin impacted the mouse brain according to the preset parameters after clicking the start button on the operating system. After the impact, the blood seepage was wiped with a sterilized cotton ball, and the incision was closed with surgical suture and sterilized with iodophor. Upon awakening, the mice were placed in their original grouped cages with sufficient water and feed at the appropriate temperature. In addition, to reduce the risk of post-traumatic intracranial infection, we ensured strict sterility of all surgical instruments and the operating environment. The surgical area was treated with disinfectant, and sterile gloves and masks were worn. The mice were kept in a clean living environment with regular bedding changes and provided with sufficient food and water. The behaviour and health of the mice were closely monitored. After surgery, sterile dressings were used to cover the wounds, and the wound healing process was regularly inspected to prevent infection. The temperature and humidity were maintained at appropriate levels to avoid the risk of infection caused by environmental factors.

C57BL/6 mice were divided into three groups: sham group ( $n = 7$ ), Model group ( $n = 7$ ), Model + Irisin group ( $n = 7$ ). Two mice died in the model group and the model + irisin group, respectively, and we added seven more. The survival rate of the model group and the model + irisin group was 88%. The sham group had a 100% survival rate. The model + Irisin group was injected intraperitoneally with irisin (100  $\mu\text{g/kg}$ ) 2 h after modeling for 7 consecutive days. And we observed the brain damage in mice from the seventh day.

C57BL/6 mice were divided into five groups: sham group, Model group, Model + Irisin-L group, Model + Irisin-H group, Model + AICAR (AMPK agonist) group. 10 pieces per group. The model + Irisin-L group was injected intraperitoneally with irisin (50  $\mu\text{g/kg}$ ) 2 h after modeling for 7 consecutive days. The model + Irisin-H group was injected intraperitoneally with irisin (100  $\mu\text{g/kg}$ ) 2 h after modeling for 7 consecutive days. Model + AICAR was administered by intraperitoneal injection of AICAR (0.5 mg/g) 2 h after modeling, once daily for 7 days. And we observed the brain damage in mice from the first day, the third day and the seventh day. The number and survival rate of mice in each group observed on the first day were sham group (10, 100%), Model group (9, 90%), Model + Irisin-L group (8, 80%), Model + Irisin-H group (9, 90%), Model + AICAR group (9, 90%). The number and survival rate of mice in each group observed on the third day were sham group (10, 100%), Model group (8, 80%), Model + Irisin-L group (8, 80%), Model + Irisin-H group (8, 80%), and Model + AICAR group (9, 90%). The number and survival rate of mice in each group observed on the seventh day were

sham group (10, 100%), Model group (7, 70%), Model + Irisin-L group (8, 80%), Model + Irisin-H group (9, 90%), and Model + AICAR group (9, 90%).

### Morris water maze test

**Learning Ability Test:** The mice were placed at an entry point in the water, and the time it took for them to swim to the platform was recorded, which was considered the escape latency. If the mice did not reach the platform within 2 min, they were guided to the platform. The mice were trained for 5 consecutive days, and the escape latency was recorded on the 6th day.

**Spatial Memory Ability Test:** On the 7th day, the platform was removed, and the farthest point from where the platform had been was designated as the entry point. The number of times the mice crossed the platform area within 2 min was observed.

### Sample collection

After completing the Morris water maze test, the mice were euthanized using CO<sub>2</sub>. Brain tissues were collected and divided into two parts: one part was fixed in 4% paraformaldehyde, and the other was stored frozen at −80 °C.

### TUNEL fluorescence

The injured brain tissues fixed in 4% paraformaldehyde, as obtained in “1.4,” were prepared into paraffin sections. The paraffin sections were deparaffinized using xylene and hydrated with a graded ethanol series. Then, the TUNEL kit was used to detect apoptotic neurons, which were observed and photographed under an optical microscope. Normal nuclei appeared blue, while apoptotic positive cells showed green fluorescence. Fluorescence microscopy was used and apoptotic cells fluoresced green and nuclei fluoresced blue.

### Nissl staining

The paraffin sections from “1.5” were deparaffinized, dehydrated with a graded ethanol series, and then placed in distilled water. The sections were stained with cresyl violet solution for 30 min (stained in an incubator at 37 °C for 10 min), then washed with distilled water, differentiated with 95% ethanol solution, and observed under a microscope. Nissl bodies appeared purple, cell nuclei were light purple, and glial cells were light purple. The sections were dehydrated with absolute ethanol, cleared with xylene, and mounted for observation under a light microscope. Under the optical microscope, hippocampal neurons were observed, with clear boundaries for pyramidal neurons, and the number of surviving neurons in the CA1 region of the hippocampus was counted. Observation using a light microscope was used.

### HE staining

Brain tissues from mice in the sham group, Model group, Model + Irisin-L group, Model + Irisin-H group, Model + AICAR group, which were fixed in 4% paraformaldehyde, are selected and renamed as the sham group, Model group, Model + Irisin-L group, Model + Irisin-H group, Model + AICAR group, respectively. The tissues were then embedded in paraffin and cut into 4 µm thick sections. After deparaffinization, rehydration, counterstaining, and clearing, the sections were stained with HE. Finally, the sections were observed, and images were captured under an optical microscope. The damage area was calculated using imageJ.

### Western blot detection

50–100 mg of brain tissue was collected from the Model group and Model + Irisin group mice. The tissues were rinsed in pre-cooled saline, and kidney tissue proteins were extracted using RIPA lysis buffer. The tissue was ground using a high-throughput freezing tissue grinder, lysed on ice for 30 min, and centrifuged at 12,000 r/min at 4 °C for 10 min. The supernatant was collected, and protein concentration was determined by the BCA method. Electrophoresis was performed, and the proteins were transferred to a PVDF membrane for 2 h. The membrane was blocked with gentle shaking at room temperature for 2 h, washed 3 times with TBST, and then incubated with the primary antibody (p-AMPK (ab133448, Abcam, 1:1000); p-MerTK (ab192649, Abcam, 1:1000); p-SYK (ab62338, Abcam, 1:1000); FcγR (ab313849, Abcam, 1:1000); NOX4 (MA5-32090, Thermo Fisher, 1:1000); Dectin-1 (ab217331, Abcam, 1:1000); PGC-1α (ab313559, Abcam, 1:1000); KLF-4 (ab214666, Abcam, 1:1000); Iba1 (ab178847, Abcam, 1:1000); NLRP3 (ab263899, Abcam, 1:1000); Arginase-1 (#93668, CST, 1:1000); GAPDH (ab9485, Abcam, 1:2500)) on a shaker at room temperature for 1 h, followed by overnight incubation at 4 °C on a shaker. The next day, the membrane was incubated at room temperature on a shaker for 0.5 h, washed 3 times (8 min each), and then incubated with the secondary antibody (ab6721, Abcam) diluted 1:2000 in TBST at room temperature on a shaker for 2 h. The ECL method was used for detection. The band grayscale values were analyzed using ImageJ software, and the relative expression level of the target protein was calculated as the grayscale value of the target protein divided by the grayscale value of the internal reference protein GAPDH.

### Cell grouping

Mouse microglia BV2 cells were purchased from Procell. BV2 cells were divided into seven groups as follows: NC group, RBC group, BV2 cells were cultured in 1% O<sub>2</sub>, glucose concentration of 0.5 g/L (2.8 mM), 1–2% fetal bovine serum medium with 100 µL of 5% mouse erythrocyte suspension, and placed in a CO<sub>2</sub> incubator for 1 ~ 3 h. RBC + Irisin group, BV2 cells were cultured in 1% O<sub>2</sub>, glucose concentration of 0.5 g/L (2.8 mM) and 1–2% fetal bovine serum medium with 100 µL of 5% mouse erythrocyte suspension, and placed in a CO<sub>2</sub> incubator for 1 ~ 3 h. RBC + Irisin group, cells were cultured according to RBC group was stimulated and treated with Irisin at a concentration of 5 ng/mL. RBC + AICAR group was stimulated and treated with AMPK agonist AICAR at a

concentration of 2.0 mmol/L according to RBC group. RBC + Irisin + AICAR group was stimulated and treated with AMPK agonist AICAR (2.0 mmol/L, HY-13417, MCE) according to RBC group. AICAR stimulation (2.0 mmol/L). RBC + AICAR + UNC2541 group, treated according to the RBC + AICAR group and subjected to the MerTK inhibitor UNC2541 (2.5  $\mu$ M, HY-125510, MCE). RBC + Irisin + AICAR + UNC2541 group, treated according to the RBC + Irisin + AICAR group was treated and stimulated by MerTK inhibitor UNC2541 (2.5  $\mu$ M). BV2 from NC group, RBC group, RBC + Irisin group, RBC + AICAR group, RBC + Irisin + AICAR group, RBC + AICAR + UNC2541 group and RBC + Irisin + AICAR + UNC2541 group, respectively. Cells were assayed for protein expression according to the experimental procedure in “1.4”.

### Q-PCR assay

Seven groups of BV2 cells were collected, and Trizol was added. The TakaRa reagent kit PrimeScript<sup>TM</sup>RT reagent Kit with gDNA Eraser (Perfect Real Time) and the SYBR Green I method were used. The steps of de-DNA reaction, reverse transcription, and the preparation of the reaction system were strictly followed, and finally, the data were obtained on the machine. YM-1: Forward: 5'-ATG AAG CAT TGA ATG GTC TGA AAG-3'; Reverse: 5'-TGA ATA TCT GAC GGT TCT GAG GAG-3'. Arginase-1: Forward: 5'-TGA CTG AAG TAG ACA AGC TGG GGA T-3'; Reverse: 5'-CGA CAT CAA AGC TCA GGT GAA TCG G-3'. FIZZ: Forward: 5'-AGG TCA AGG AAC TTC TTG CCA ATC C-3'; Reverse: 5'-AAG CAC ACC CAG TAG CAG TCA TCC C-3'. IL-1 $\beta$ : Forward: 5'-CAG GCA GGC AGT ATC ACT CA-3'; Reverse: 5'-TGT CCT CAT CCT GGA AGG TC-3'. IL-1 $\beta$ : Forward: 5'-CAG GCA GGC AGT ATC ACT CA-3'; Reverse: 5'-TGT CCT CAT CCT GGA AGG TC-3'. NLRP3: Forward: 5'-GTG GAG ATC CTA GGT TTC TCT G-3'; Reverse: 5'-CAG GAT CTC ATT CTC TTG GAT C-3'. TNF $\alpha$ : Forward: 5'-CCC ACG TCG TAG CAA ACC A-3'; Reverse: 5'-CCG TTG GCC AGG AGG GCG TTG-3'. HMGB1: Forward: 5'-AGG AGT GGC TTT TGT CCC TC-3'; Reverse: 5'-AGA GGC CGC AGT TTC CTA TC-3'. Galectin-3: Forward: 5'-AGA CAG CTT TTC GCT TAA CGA-3'; Reverse: 5'-GGG TAG GCA CTA GGA GGA GC-3'. Caspase-1: Forward: 5'-GTG TTG CAG ATA ATG AGG GC-3'; Reverse: 5'-AAG ATC CTG AGG GCA AAG AG-3'. Caspase-4: Forward: 5'-TGT CTC ATG GCA CAC TGC AT-3'; Reverse: 5'-AGG CCT GCA CAA TGA TGA CT-3'. GSDMD: Forward: 5'-TGC AGT GTC TGA CAG TTC CAG-3'; Reverse: 5'-AAC AGG TCA TCC CCA CGA CT-3'. GAPDH: Forward: 5'-GGT TGT CTC CTG CGA CTT CA-3'; Reverse: 5'-TGG TCC AGG GTT TCT TAC TCC-3'.

### ELISA

The cell supernatant from Sect. 1.9 was collected, and the levels of cGAMP (EiAGAMP, Thermo Fisher), IL-1 $\beta$  (PI301, Beyotime), TNF- $\alpha$  (PT512, Beyotime), MDA (E-EL-0060, Elabscience), SOD (S0101S, Beyotime) and GSH (S0053, Beyotime) in the cell supernatant of each group were measured following the instructions provided with the ELISA kit.

### Flow apoptosis

Logarithmic growth stage BV2 cells were taken, and  $2 \times 10^5$  cells/well (1640 medium containing 1% serum) were inoculated in a 6-well plate. The supernatant of seven groups of cells stimulated by different treatments was collected into a centrifuge tube. After digestion of adherent cells, the cell suspension was similarly collected, merged with the cell supernatant, and centrifuged. The supernatant was discarded. FITC and PI dye were added and combined in accordance with the Apoptosis Detection Kit's instructions. The reaction was then allowed to proceed for 20 min at room temperature while being shielded from light. Flow cytometry was used to identify apoptosis.

### Statistical analysis

GraphPad 9.0 was used for charting, while SPSS 23.0 was utilised for statistical analysis. The measurement data were presented as  $x \pm s$ , and the paired or unpaired Student's *t* test (parametric or non-parametric test) was used to analyse the differences between the two groups. The findings were statistically significant, and a difference of  $p < 0.05$  was deemed significant. (\* $P < 0.05$ ; \*\* $P < 0.01$ ).

## Results

### Raw letter analysis

44 highly expressed genes and 30 lowly expressed genes were screened by limma package analysis in brain trauma after 4 h; 31 highly expressed and 11 lowly expressed in brain trauma after 24 h. ClusterProfiler's GO and KEGG analysis showed that DEGs were substantially enriched in a number of biological pathways. After 4 h, GO analysis in brain trauma demonstrated that DEGs were significantly enriched in biological processes like receptor ligand activity and signalling receptor activator activity. KEGG pathway analysis also showed that DEGs were significantly enriched in the NF- $\kappa$ B and MAPK signalling pathways; GO analysis in brain trauma after 24 h revealed that DEGs were significantly enriched in the NADPH oxidase complex, perinuclear endoplasmic reticulum and response to corticosteroid (Fig. 1).

### Irisin improves behavior as well as the extent of injury in mice with traumatic brain injury

After the mouse model was successfully established, in the Morris water maze test, compared with the sham group, the escape latency of the model group mice was significantly increased, and the time in the target quadrant was significantly reduced. In contrast, the model + Irisin group's escape latency was substantially lower and their stay in the target quadrant was significantly longer than that of the model group (Fig. 2A).

TUNEL staining results showed that compared with the sham group, the number of TUNEL-positive cells in the model group and the model + Irisin group was significantly increased. There were much fewer TUNEL-positive cells in the model + Irisin group than in the model group. Nissl staining revealed that the model group's



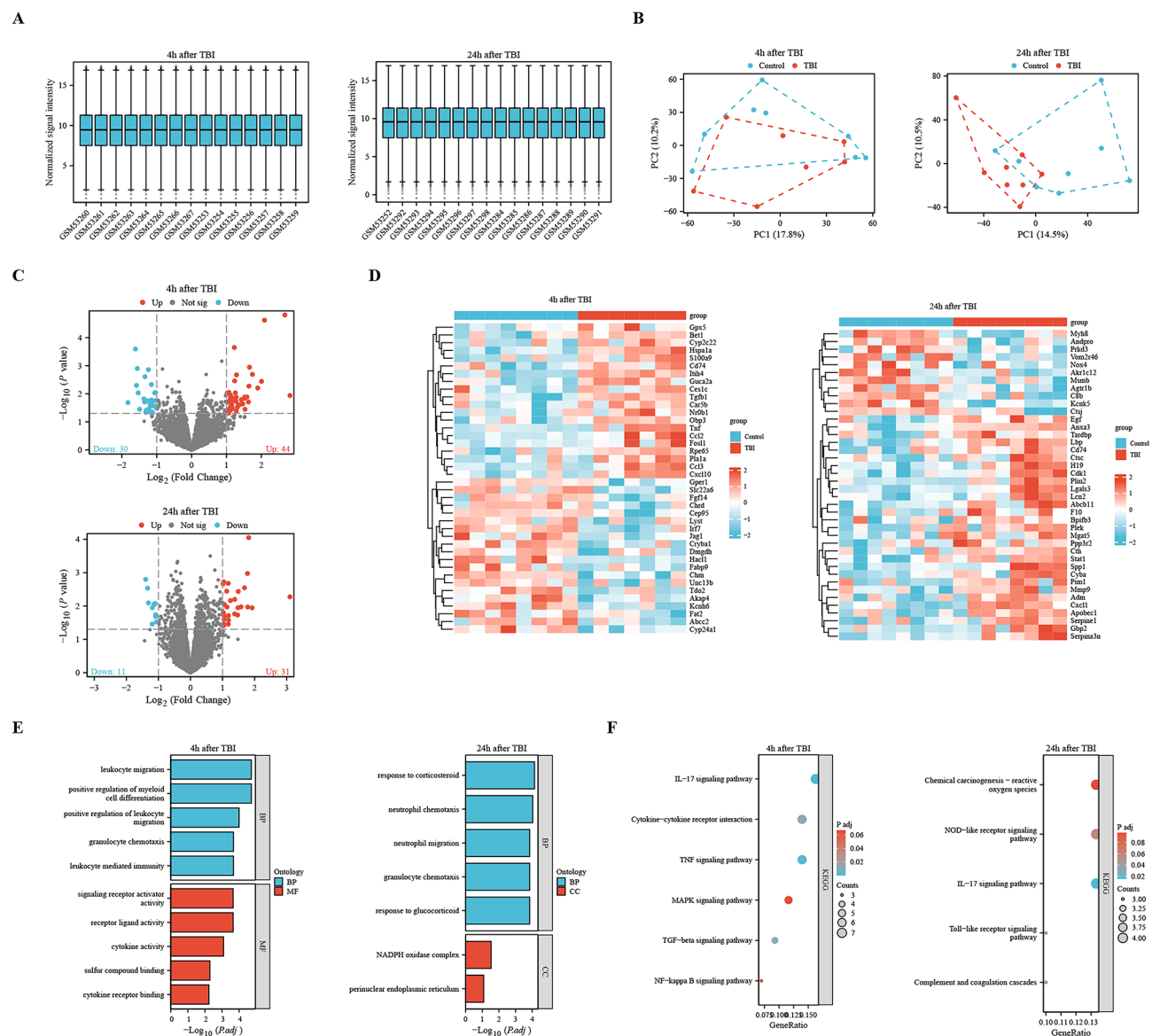


**Fig. 1.** Bioinformatics analysis. (A) Box plots of sample calibration at 4 h and 24 h; (B) PCA plots showing sample differences at 4 h and 24 h; (C) Volcano plots of differential genes at 4 h and 24 h; (D) Heatmaps of differential genes at 4 h and 24 h; (E) Bar charts of GO enrichment analysis at 4 h and 24 h; (F) Bubble plots of KEGG enrichment analysis at 4 h and 24 h.

hippocampus neurones were significantly injured in the sham group, as seen by uneven cell bodies, cell atrophy, and darkly stained nuclei. However, the number of damaged hippocampal neurones in the model + Irisin group was reduced, and the degree of damage was alleviated. This indicates that Irisin can reduce the damage caused by traumatic brain injury to a certain extent (Fig. 2B).

Observation and HE staining of mouse brain tissue showed that on the seventh day, the area of brain damage was significantly higher in the model group compared to the sham group. In contrast, the area of brain damage was significantly lower in the model + Irisin-L group, model + Irisin-H group and model + AICAR group compared to the model group. And the area of brain damage was significantly lower in the model + Irisin-H group and model + AICAR group compared to the model + Irisin-L group. There was no significant difference in the brain injury area between the model + Irisin-H group and the model + AICAR group. The brain injury area of the model group gradually increased from day 1 to day 7. The brain injury area of the model + Irisin-L group, model + Irisin-H group and model + AICAR group gradually decreased from day 1 to day 7 (Fig. 3A, B).

According to the findings of the Western blot, the model group's relative levels of NLRP3 and Arginase-1 protein expression were considerably greater and lower, respectively, than those of the sham group. While the relative protein expression levels of Arginase-1 were considerably greater than those of the model group, the relative protein expression levels of NLRP3 were significantly lower in the model + Irisin-L, model + Irisin-H, and model + AICAR groups than in the model group. The model + Irisin-H and model + AICAR groups had

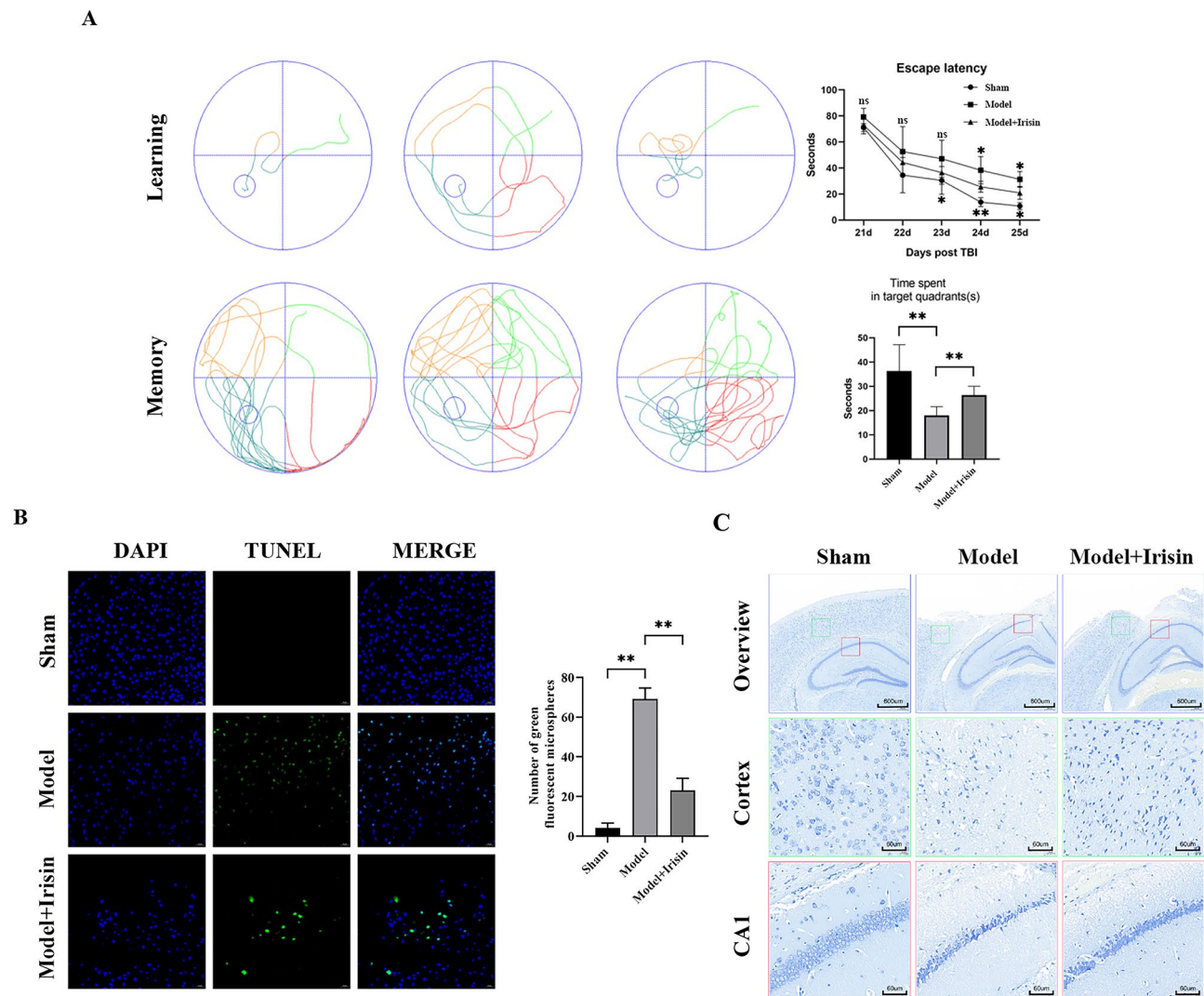


**Fig. 2.** Irisin improve behavioral ability and brain damage in mice with TBI. **(A)** Morris water maze test to assess the learning and spatial memory abilities of mice in the sham group, Model group, and Model + Irisin group; **(B)** TUNEL fluorescence detection of cell apoptosis in the brain tissues of the sham group, Model group, and Model + Irisin group; **(C)** Nissl staining to assess hippocampal neuron survival in the sham group, Model group, and Model + Irisin group. \*\* $P < 0.01$ ; \* $P < 0.05$ ;  $n_s P > 0.05$ .

considerably lower relative protein expression levels of NLRP3 than the model + Irisin-L group, whereas the model + Arginase-1 group had significantly higher relative protein expression levels. The model + Irisin-H group and the model + AICAR group did not significantly vary in the relative levels of NLRP3 and Arginase-1 protein expression. There was also no significant difference in the relative protein expression levels of Iba1 between the groups (Fig. 4A).

The model group's relative mRNA expression levels of HMGB1 and Galectin-3 were considerably greater than those of the sham group, according to subsequent Q-PCR data. The relative mRNA expression levels of HMGB1 and Galectin-3 were considerably lower in the model + irisin-L, model + irisin-H, and model + AICAR groups than in the model group. The relative mRNA expression levels of HMGB1 and Galectin-3 were considerably lower in the model + irisin-H group and the model + AICAR group than in the model + irisin-L group. The model + irisin-H group and the model + AICAR group did not significantly vary in the relative mRNA expression levels of HMGB1 and Galectin-3 (Fig. 4B). ELISA results showed that the concentration of cGAMP in the model group was significantly higher than that in the sham group. Compared with the model group, the concentrations of cGAMP were significantly lower in the model + irisin-L group, the model + irisin-H group and the model + AICAR group. Compared with the model + irisin-L group, the concentrations of cGAMP in the model + irisin-H group and the model + AICAR group were significantly lower. There was no significant difference in the concentration of cGAMP in the model + irisin-H group and the model + AICAR group (Fig. 4C).

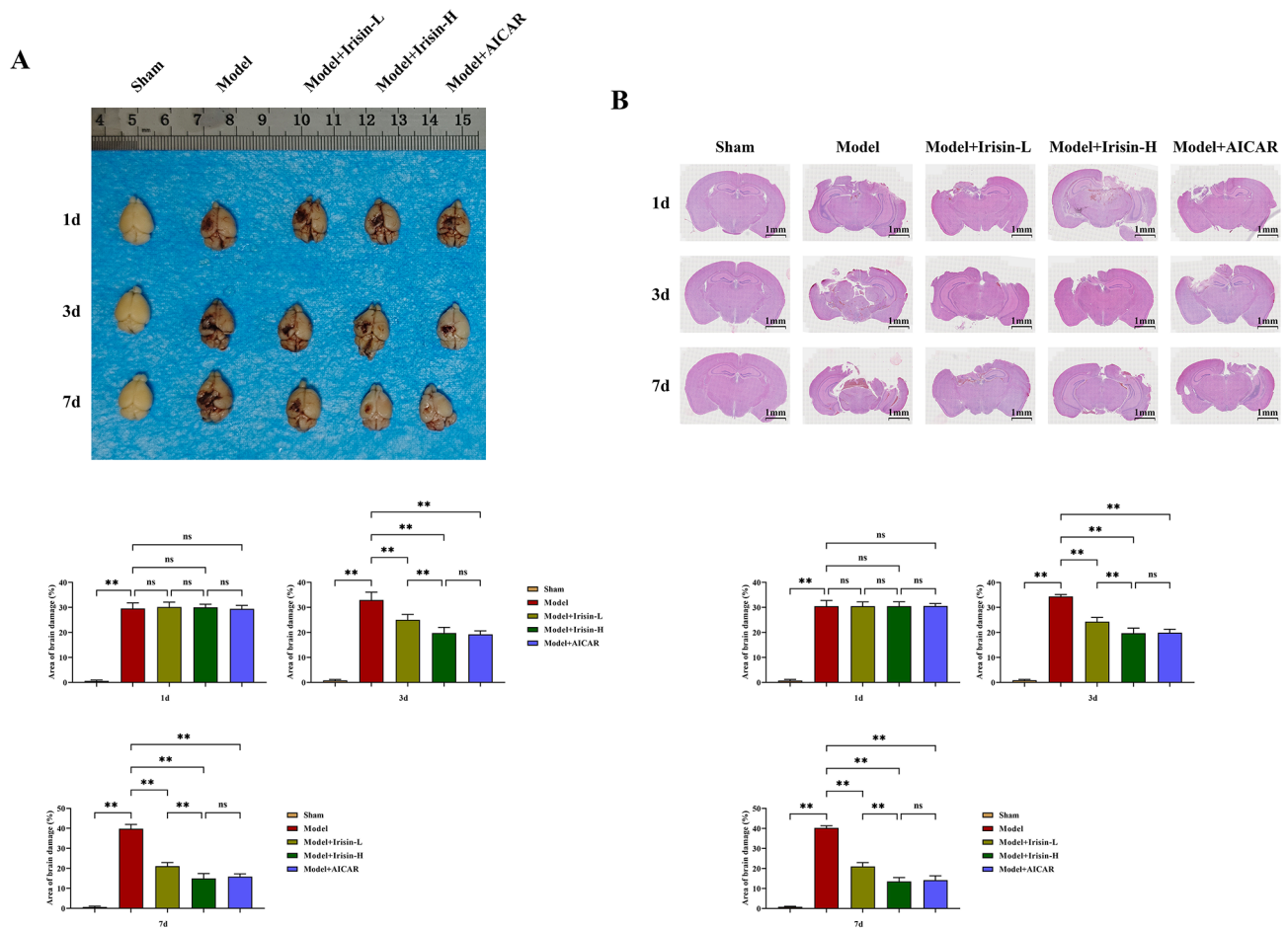


**Fig. 3.** Irisin significantly reduces damage caused by TBI. (A) Observation of brain tissue specimens from the sham group, Model group, Model + Irisin-L group, Model + Irisin-H group, Model + AICAR group mice; (B) HE staining to observe neuronal damage in the brain tissues of the sham group, Model group, Model + Irisin-L group, Model + Irisin-H group, Model + AICAR group mice. Data are expressed as the mean  $\pm$  standard deviation. \*\* $P < 0.01$ ; \* $P < 0.05$ ; ns $P > 0.05$ .

### Irisin promotes AMPK and MerTK phosphorylation

Western blot results showed that compared with the model group, the relative protein levels of p-AMPK and p-MerTK were significantly increased, while the relative protein levels of p-SYK and FcγR were significantly decreased in the model + irisin group. This suggested that irisin promoted the phosphorylation of AMPK and MerTK (Fig. 5).

### Irisin increases expression of phosphorylated AMPK and phosphorylated MerTK, promotes autophagy, and inhibits Thermoprotein deposition/inflammatory response

According to Western blot data, the RBC group's relative expression levels of p-AMPK, PGC-1 $\alpha$ , and KLF4 were substantially lower than those of the NC group, but the RBC group's relative expression levels of p-MerTK, LC3I, Beclin-1, NOX4, p-SYK, and Dectin-1 were significantly greater. The relative expression levels of p-AMPK, PGC-1 $\alpha$ , KLF4, p-SYK, and Dectin-1 were considerably higher than those of the RBC group. However, there was a considerable drop in the relative expression levels of Dectin-1, p-SYK, and NOX4. Relative expression levels of NOX4, p-SYK, and Dectin-1 were considerably lower in the RBC + AICAR group than in the RBC group, although the relative expression levels of p-AMPK, PGC-1 $\alpha$ , KLF4, p-MerTK, LC3I, and Beclin-1 were significantly higher. In the RBC + Irisin + AICAR group, the relative expression levels of NOX4, p-SYK, and Dectin-1 were substantially lower than those of the RBC + Irisin group, whereas the relative expression levels of p-AMPK, PGC-1 $\alpha$ , KLF4, p-MerTK, LC3I, and Beclin-1 were significantly higher. The relative expression levels of p-AMPK, PGC-1 $\alpha$ , KLF4, LC3I, and Beclin-1 did not vary substantially from the RBC + AICAR + UNC2541 group, but the relative expression level of p-MerTK was considerably lower. Relative expression levels of Dectin-1, p-SYK, and NOX4 were elevated. The RBC + Irisin + AICAR + UNC2541 group exhibited substantially reduced p-MerTK, no significant change in the relative expression levels of p-AMPK, PGC-1 $\alpha$ , KLF4, LC3I, and Beclin-1, and higher levels of NOX4, p-SYK, and Dectin-1 as compared to the RBC + Irisin + AICAR group (Fig. 6 A, B).

To determine the degree of autophagy, Q-PCR was used. The relative mRNA levels of YM-1, FIZZ, and arginase-1 in the RBC group were significantly lower than those in the NC group; the relative mRNA levels of



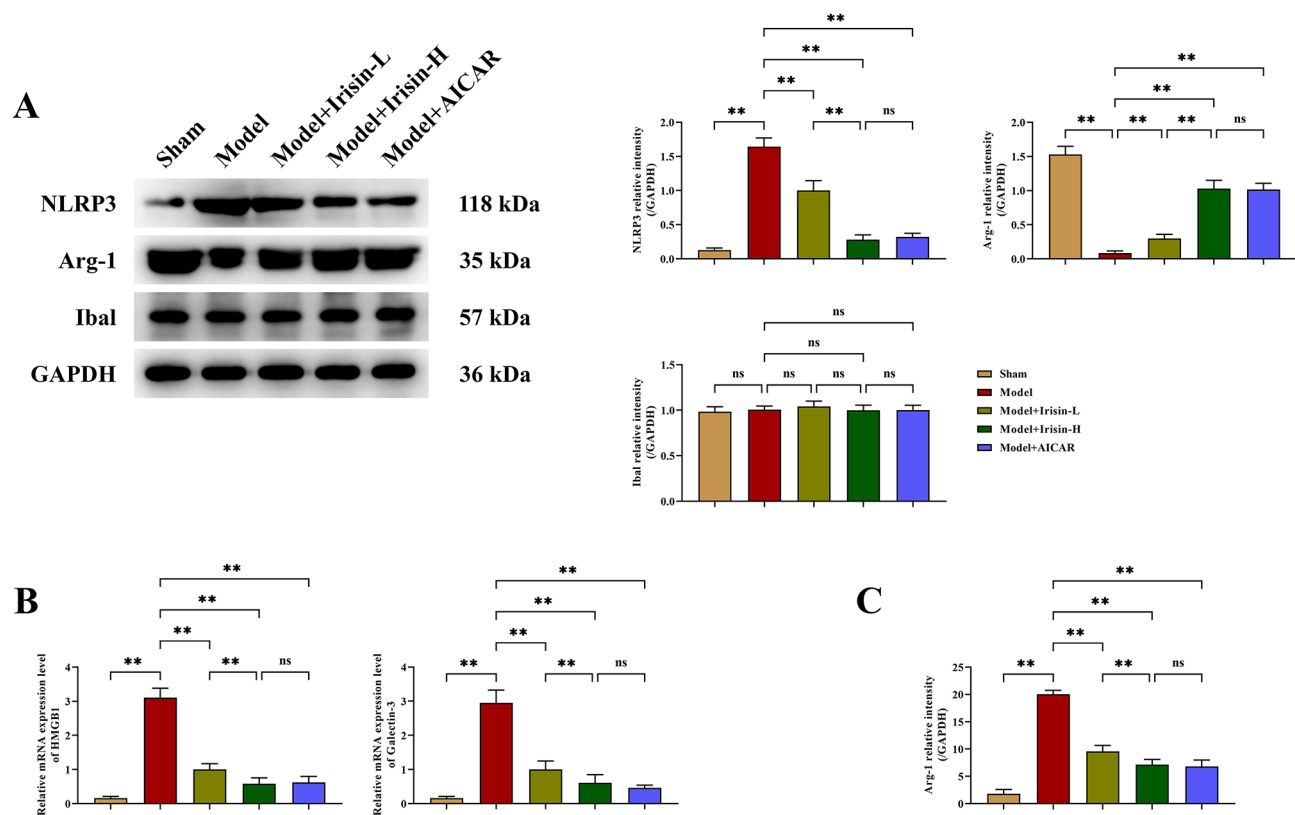


**Fig. 4.** Irisin significantly reduces damage caused by TBI. (A) Western blot detection of NLRP3, Arginase-1, and Iba1 expression in mouse brain tissue from the sham group, Model group, Model + Irisin-L group, Model + Irisin-H group, Model + AICAR group mice; (B) Q-PCR detection of HMGB1 and Galectin-3 levels in the five groups; (C) ELISA detection of cGAMP levels in the five groups. Data are expressed as the mean  $\pm$  standard deviation. \*\* $P < 0.01$ ; \* $P < 0.05$ ; ns $P > 0.05$ .

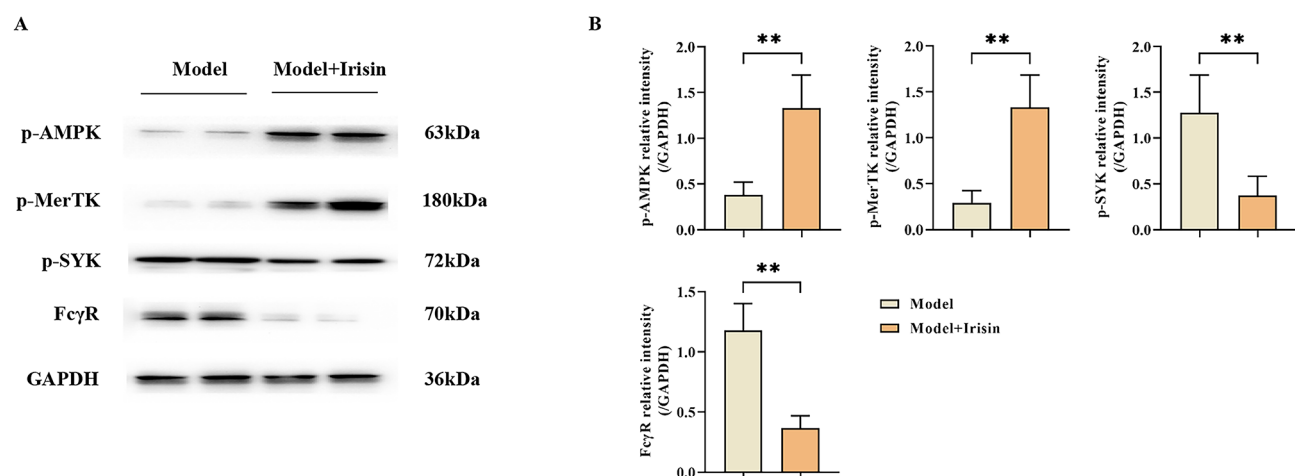


**Fig. 5.** Irisin promotes phosphorylation of AMPK and MerTK. (A) Western blot detection of p-AMPK, p-MerTK, p-SYK and FcγR protein bands in mouse brain tissue from the Model group and the Model + Irisin group; (B) Western blot statistical chart of the expression of p-AMPK, p-MerTK, p-SYK and FcγR proteins in mouse brain tissue in the Model group and the Model + Irisin group. GAPDH as control protein. Data are expressed as the mean  $\pm$  standard deviation. \*\* $P < 0.01$ ; \* $P < 0.05$ ; ns $P > 0.05$ .

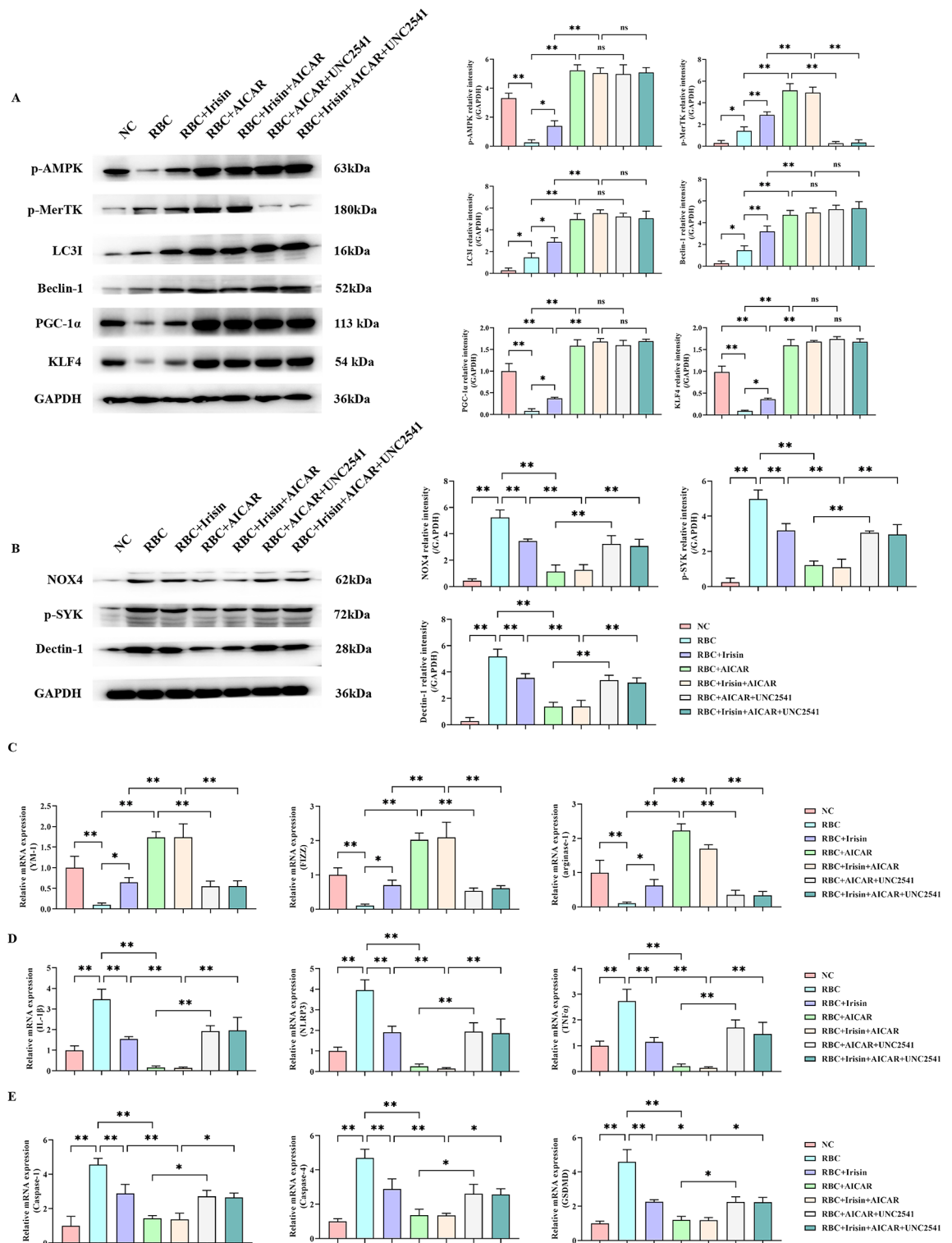


**Fig. 6.** Irisin increases the expression of phosphorylated AMPK and phosphorylated MerTK proteins, promotes autophagy, and inhibits pyroptosis/inflammatory response. **(A)** Western blot detection of p-AMPK, p-MerTK, PGC-1α, KLF4, LC3I, and Beclin-1 protein expression in BV2 cells; **(B)** Western blot detection of NOX4, p-SYK, and Dectin-1 protein expression in BV2 cells from the above seven groups; **(C)** Q-PCR detection of YM-1, FIZZ, and arginase-1 levels in the seven groups; **(D)** Q-PCR detection of NLRP3, IL-1β, and TNFα levels in the seven groups; **(E)** Q-PCR detection of Caspase-1, Caspase-4, and GSDMD levels in the seven groups. GAPDH as control protein. Data are expressed as the mean ± standard deviation. \*\* $P < 0.01$ ; \* $P < 0.05$ ; <sup>ns</sup> $P > 0.05$ .

these three genes were significantly higher in the RBC + Irisin group than in the RBC + Irisin group; and the relative mRNA levels of YM-1, FIZZ, and arginase-1 were significantly lower in the RBC + Irisin + AICAR group than in the RBC + Irisin group than in the RBC + Irisin group. The RBC + AICAR group had considerably greater relative mRNA levels of YM-1, FIZZ, and arginase-1 than the RBC group did. The RBC + AICAR + UNC2541 group had much lower relative mRNA levels of YM-1, FIZZ, and arginase-1 than the RBC + AICAR group. The RBC + Irisin + AICAR + UNC2541 group had much lower relative mRNA levels of YM-1, FIZZ, and arginase-1 than the RBC + Irisin + AICAR group (Fig. 6C).

To determine the degree of inflammation, Q-PCR was used. The relative mRNA levels of NLRP3, IL-1 $\beta$ , and TNF $\alpha$  were significantly higher in the RBC group than in the NC group; they were significantly lower in the RBC + Irisin group than in the RBC + Irisin group; and they were significantly lower in the RBC + Irisin + AICAR group than in the RBC + Irisin group when compared to the RBC + Irisin group. The RBC + AICAR group had considerably lower relative mRNA levels of NLRP3, IL-1 $\beta$ , and TNF $\alpha$  than the RBC group. The RBC + AICAR + UNC2541 group had substantially higher relative mRNA levels of NLRP3, IL-1 $\beta$ , and TNF $\alpha$  than the RBC + AICAR group. Compared with the RBC + Irisin + AICAR group, the relative mRNA levels of NLRP3, IL-1 $\beta$  and TNF $\alpha$  in the RBC + Irisin + AICAR + UNC2541 group were significantly increased (Fig. 6D).

To determine the degree of lysis, Q-PCR was used. The RBC + Irisin group had significantly lower relative mRNA levels of Caspase-1, Caspase-4, and GSDMD than the RBC + Irisin group; the RBC + Irisin + AICAR group had significantly lower relative mRNA levels of Caspase-1, Caspase-4, and GSDMD than the RBC + Irisin group; and the RBC + Irisin + AICAR group had significantly higher relative mRNA levels of Caspase-1, Caspase-4, and GSDMD than the NC group. The RBC + AICAR group had much lower relative mRNA levels of Caspase-1, Caspase-4, and GSDMD than the RBC group. The RBC + AICAR + UNC2541 group had considerably greater relative mRNA levels of Caspase-1, Caspase-4, and GSDMD than the RBC + AICAR group. The RBC + Irisin + AICAR + UNC2541 group had much greater relative mRNA levels of Caspase-1, Caspase-4, and GSDMD than the RBC + Irisin + AICAR group (Fig. 6E).

### Irisin inhibits apoptosis by modulating AMPK/MerTK and attenuates traumatic brain injury by inhibiting SYK/ROS/inflammatory signaling

When compared to the NC group in the ELISA experiment, the RBC group had higher levels of IL-1 $\beta$ , TNF $\alpha$ , and MDA and lower levels of GSH and SOD; the RBC + Irisin group had lower levels of IL-1 $\beta$ , TNF $\alpha$ , and MDA and higher levels of GSH and SOD; and the RBC + AICAR group had lower levels of IL-1 $\beta$ , TNF $\alpha$ , and MDA and higher levels of GSH and SOD; compared with the RBC + AICAR group, the RBC + Irisin + AICAR group had decreased IL-1 $\beta$ , TNF $\alpha$  and MDA levels and increased GSH and SOD levels; compared with the RBC + AICAR + UNC2541 group, the IL-1 $\beta$ , TNF $\alpha$  and MDA levels increased, and GSH and SOD levels decreased; compared with the RBC + Irisin + AICAR group, IL-1 $\beta$ , TNF $\alpha$  and MDA levels increased, and GSH and SOD levels decreased (Fig. 7A, B). According to the flow cytometry results, the NC group did not exhibit apoptosis; the RBC + Irisin group had fewer apoptotic cells than the RBC group; the RBC + AICAR group and the RBC + Irisin + AICAR group had fewer apoptotic cells than the RBC group and the RBC + Irisin group; and the RBC + AICAR + UNC2541 group and the RBC + Irisin + AICAR + UNC2541 group had more apoptotic cells than the RBC group and the RBC + Irisin + AICAR + UNC2541 group (Fig. 7C). The above results suggested that irisin inhibited the progression of traumatic brain injury by regulating AMPK/MerTK/autophagy and SYK/ROS/inflammatory signaling (Fig. 8).

## Discussion

TBI is a complex neurological disease, the incidence of which is increasing annually approximately 100,000 people die from craniocerebral injury in China, which clinically manifests as exogenous compression from mass injury, contusion, and neuronal damage caused by ischemia, apoptosis, mitochondrial dysfunction, cortical diffusion inhibition, and microvascular thrombosis<sup>31</sup>. Brain tissue hypoxia, endothelial cell injury, and inflammatory response secondary to craniocerebral injury are important factors affecting the prognosis of patients<sup>32</sup>; some proteins and factors such as insulin-like growth factor 1, fibrillar gelatin-3, neuron specific enolase and other biomarkers are related to angiogenesis, secondary ischemia, and neurological injury, and have a role in the severity of traumatic brain injury and its prognosis assessment. Therefore, it is necessary to identify the proteins and factors related to the diagnosis, treatment, and prognosis of traumatic brain injury for timely intervention.

Irisin, a muscle factor secreted by skeletal muscles during exercise, has recently been shown to play an important role in metabolic regulation and pathophysiological processes in various diseases. It possesses anti-inflammatory properties that reduce chronic inflammation, which is potentially beneficial in the prevention and treatment of many diseases. Studies have shown that Irisin exerts protective effects on the nervous system, reduces neuronal damage and cell death through various mechanisms, and has antioxidant properties that reduce neuronal damage from oxidative stress. Thus, research into the relationship between Irisin and brain injury has increased. In this study, we found that Irisin alleviated brain injury in TBI mice, inhibited apoptosis by regulating AMPK/MerTK, and alleviated TBI injury by inhibiting SYK/ROS/inflammatory signaling.

In an animal model of TBI, injecting Irisin significantly reduced apoptosis and inflammatory responses in the injured brain region and improved neurological functions. Studies suggest that irisin may activate integrin-related signaling pathways by interacting with integrin  $\alpha v \beta 3$  receptors. Irisin was found to bind to specific sites of integrin  $\alpha v \beta 3$ ; it activates downstream signaling pathways such as AMPK through integrin  $\alpha v \beta 3$ , promoting cell survival, anti-apoptotic and anti-inflammatory responses<sup>33</sup>. AMPK (AMP-activated protein kinase (AMPK)) is a sensor of cellular energy status that, when activated, can regulate multiple metabolic and cell survival pathways through phosphorylation. SIRT1 (Sirtuin 1) is a NAD<sup>+</sup>-dependent deacetylase involved in the regulation of cellular metabolism, lifespan, and anti-stress responses. AMPK can activate SIRT1 indirectly by regulating NAD<sup>+</sup> levels or directly affect SIRT1 activity by phosphorylating upstream regulators. AMPK and

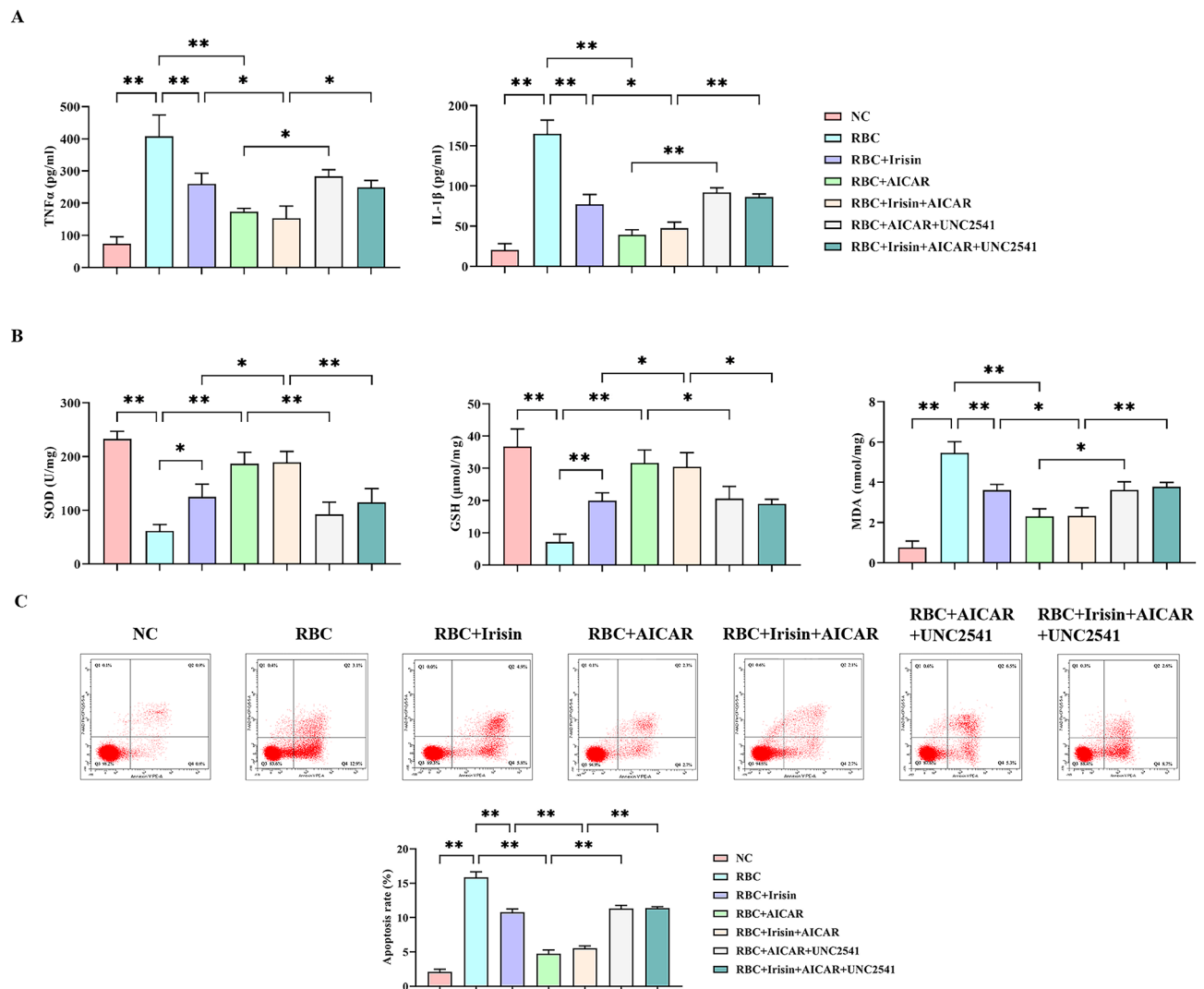


**Fig. 7.** Irisin alleviates TBI-induced damage by regulating AMPK/MerTK to inhibit apoptosis and by suppressing SYK/ROS/inflammatory signaling pathways. (A) ELISA detection of IL-1 $\beta$  and TNF $\alpha$  levels in the seven groups; (B) ELISA detection of MDA, GSH, and SOD levels in the seven groups; (C) Flow cytometry detection of apoptosis in BV2 cells in the seven groups. Data are expressed as the mean  $\pm$  standard deviation. \*\* $P < 0.01$ ; \* $P < 0.05$ .

SIRT1 work together to regulate metabolism and the cellular stress response. PGC-1 $\alpha$  is a NAD $^{+}$ -dependent deacetylase involved in the regulation of cellular metabolism and anti-stress responses. PGC-1 $\alpha$  is also a key metabolic regulator of mitochondrial biogenesis and energy metabolism. SIRT1 deacetylates and activates PGC-1 $\alpha$  and enhances its ability to regulate mitochondrial biogenesis, anti-oxidative stress, and metabolism. KLF4 (Kruppel-like factor 4) is a transcription factor involved in the regulation of cell differentiation, proliferation, and survival. PGC-1 $\alpha$  can promote the expression of KLF4 gene through activation of specific transcription factors and signaling pathways, thus affecting cell metabolism and anti-stress response. AMPK can in turn promote KLF4 activity by directly phosphorylating KLF4 or indirectly through upstream regulators. After activation, AMPK can regulate the expression and function of KLF4 through a variety of pathways. MerTK (Mer Tyrosine Kinase) is a receptor tyrosine kinase involved in cell survival, phagocytosis, and anti-inflammatory responses. KLF4, as a transcription factor, can directly or indirectly promote the expression of the MerTK gene and enhance its role in cellular clearance of apoptotic cells and in anti-inflammatory responses. AMPK, through the activation of ULK1 (Unc-51 Like Autophagy Activating Kinase 1) and other autophagy-related proteins, may promote the autophagy process and help cells to remove damaged organelles and proteins. AMPK reduces intracellular oxidative stress and protects cells from oxidative damage through activation of anti-oxidative stress-related signaling pathways (e.g., Nrf2).

Specific recognition of PtdSer by early apoptotic cells is a decisive step in initiating downstream signal-directed phagocytosis. Many receptors play a role in the tethering of apoptotic cells via two main mechanisms: direct binding to PtdSer and indirect binding via soluble bridging molecules. PtdSer receptors that bind directly include the brain-specific angiogenesis inhibitor 1 (BAI-1)<sup>34</sup>, T-cell immunoglobulin, mucin structural domain-



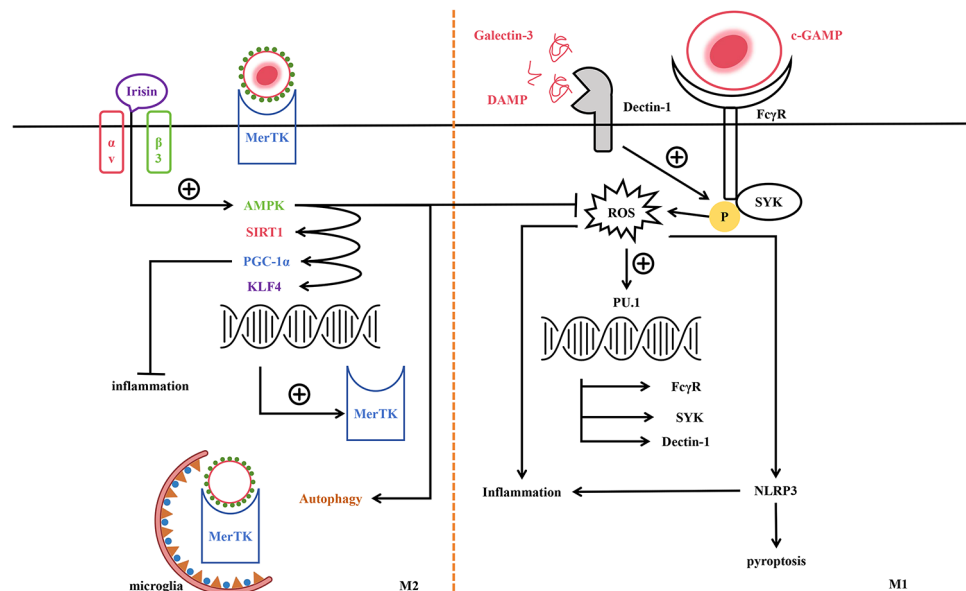


**Fig. 8.** Irisin inhibits the progression of traumatic brain injury by regulating AMPK/MerTK/autophagy and SYK/ROS/inflammatory signaling pathways.

containing protein 4 (Tim4), and atypical epidermal growth factor (EGF) motifs that contain stabilizing proteins –1 and –2<sup>35,36</sup>. In contrast, MerTK binds to PtdSer by binding to specific bridging proteins, such as Gas6 (Growth Arrest-Specific 6) or Protein S. When apoptotic cells are exposed to PtdSer, bridging proteins such as Gas6 or Protein S bind to PtdSer. Subsequently, these bridging proteins bind to the MerTK receptor via another structural domain to activate MerTK<sup>37</sup>. Activation of the MerTK receptor triggers a downstream signaling pathway that results in phagocytosis of the apoptotic cell by phagocytes. This mechanism ensures that apoptotic cells are efficiently removed, thereby preventing the release of harmful substances and triggering of inflammatory responses.

In vitro experiments have shown that BV2 microglial cells are stimulated by red blood cells. When red blood cells are destroyed or undergo apoptosis, their contents are released into the extracellular environment. cGAMP is a cyclic dinucleotide that is normally produced in the cytoplasm by the cGAS (cyclic GMP-AMP synthase) enzyme in response to DNA damage or exogenous DNA. In TBI, damage to neurons and glial cells can cause nuclear or mitochondrial DNA to leak into the cytoplasm, thereby activating cGAS and generating cGAMP. DAMPs are intracellular substances released into the extracellular space during cell injury or death. HMGB1 is one of many DAMPs. When the body is damaged, it is released from the cell into the extracellular space, where it is recognized by the immune system as a danger signal, triggering downstream immune responses and inflammatory cascades. In TBI, mechanical damage or necrosis of neurons and glial cells leads to the release of DAMPs, such as HMGB1, S100 proteins, ATP, and DNA. Galectin-3 is a  $\beta$ -galactoside-binding protein that is mainly secreted by activated microglia and macrophages in TBI. Its expression has been shown to be significantly upregulated in both inflammatory and injury environments. This in turn stimulates Dectin-1 and Fc $\gamma$ R. Dectin-1 is a C-type lectin-like receptor involved in the recognition of pathogens and cellular debris. Fc $\gamma$ R is a class of receptor on the surface of immune cells capable of binding to the antibody's Fc segments, which are involved in the clearance of immune complexes. Upon activation, Dectin-1 and Fc $\gamma$ R recruit and phosphorylate SYK (spleen tyrosine kinase) through its ITAM structural domain (immunoreceptor tyrosine activation motif). Phosphorylated SYK promotes the production of reactive oxygen species (ROS) through downstream signaling pathways (e.g., NF- $\kappa$ B and MAPK), leading to oxidative stress. ROS oxidative stress activates HSF1 (Heat Shock Factor 1), a major regulator of the heat shock response. Activation of HSF1 promotes the expression of SPI1, also known as PU.1. PU.1 is an important transcription factor for myeloid cell differentiation. PU.1 promotes the gene transcription of Dectin-1, Fc $\gamma$ R and SYK, thereby enhancing the expression of these receptors and kinases and further amplifying the signaling pathway. ROS not only plays a role in antimicrobial and antiviral defenses, but also induces and exacerbates inflammatory responses. ROS promotes NLRP3 (NOD-like receptor family pyrin domain containing NOD-like receptor), a major regulator of heat shock response<sup>8–15</sup>. ROS also promotes the activation of NLRP3, a multi-protein complex involved in cellular pyroptosis (inflammatory cell death) and pro-inflammatory cytokine production.

Both in vivo and in vitro experiments have shown that cGAMP, DAMP, and Galectin-3 are produced in TBI environments. cGAMP, DAMP, and Galectin-3 can mediate the recruitment of Dectin-1 and Fc $\gamma$ R and phosphorylate SYK, thereby promoting oxidative stress. ROS also promotes inflammatory responses and apoptosis. ROS can also promote Dectin-1, Fc $\gamma$ R, and SYK through PU.1, thereby exacerbating the above process. Irisin can mediate  $\alpha$ v $\beta$ 3 to promote the phosphorylation of AMPK, which can play a role in inhibiting the inflammatory response by inhibiting oxidative stress and promoting the activation of SIRT1, PGC-1 $\alpha$ , KLF4,

and MerTK. Additionally, AMPK can promote the M2 polarization of microglia and inhibit the inflammatory response and apoptosis caused by cGAMP, DAMP, and Galectin-3.

In summary, irisin inhibits the progression of traumatic brain injury by regulating AMPK/MerTK/autophagy and SYK/ROS/inflammatory signaling, providing new treatment ideas and targets for the treatment of TBI. The 7-day TBI experiment chosen for this study was primarily based on observations of acute pathological responses (e.g., inflammation, oxidative stress, and blood-brain barrier disruption), assessment of the effects of short-term interventions, and experimental cycle and resource constraints. However, such short-term experiments have limitations compared to established animal models of TBI, including the inability to assess long-term pathological changes (such as neurodegeneration and chronic inflammation), the lack of a comprehensive assessment of behavioral recovery, and the potential to underestimate the therapeutic effect. Therefore, our follow-up experiments still need to be tested in established mouse models of TBI and clinical trials to provide a strong basis for the research conclusions.

## Data availability

The data that support the findings of this study are available on request from the corresponding author.

Received: 28 August 2024; Accepted: 24 April 2025

Published online: 04 May 2025

## References

- ALOUANI A T, E. L. F. O. U. L. Y. T. Traumatic brain injury (TBI) detection: past, present, and future [J]. *Biomedicines*, **10**(10). (2022).
- FESHARAKI-ZADEH A, DATTA, D. An overview of preclinical models of traumatic brain injury (TBI): relevance to pathophysiological mechanisms [J]. *Front. Cell. Neurosci.* **18**, 1371213 (2024).
- MCGINN M J, POVISHOCK, J. T. Pathophysiology of traumatic brain injury [J]. *Neurosurg. Clin. North Am.* **27** (4), 397–407 (2016).
- HUIJBEN, J. A. et al. Variation in general supportive and preventive intensive care management of traumatic brain injury: a survey in 66 neurotrauma centers participating in the collaborative European neurotrauma effectiveness research in traumatic brain injury (CENTER-TBI) study [J]. (2018). Critical care (London, England), **22**(1): 90 .
- FANN, J. R. et al. Long-term risk of dementia among people with traumatic brain injury in Denmark: a population-based observational cohort study [J]. *Lancet Psychiatry*. **5** (5), 424–431 (2018).
- THAPA, K. et al. Traumatic brain injury: mechanistic insight on pathophysiology and potential therapeutic targets [J]. *J. Mol. Neuroscience: MN*. **71** (9), 1725–1742 (2021).
- AFONINA, I. S. et al. Limiting inflammation-the negative regulation of NF- $\kappa$ B and the NLRP3 inflammasome [J]. *Nat. Immunol.* **18** (8), 861–869 (2017).
- YANG, Q. et al. Metabolic regulation of inflammasomes in inflammation [J]. *Immunology* **157** (2), 95–109 (2019).
- FERNANDES F P et al. Inflammasome genetics and complex diseases: a comprehensive review [J]. *Eur. J. Hum. Genetics: EJHG*. **28** (10), 1307–1321 (2020).
- QIN, J. D. et al. Effect of ammonium pyrrolidine dithiocarbamate (PDTC) on NF- $\kappa$ B activation and CYP2E1 content of rats with immunological liver injury [J]. *Pharm. Biol.* **52** (11), 1460–1466 (2014).
- SWANSON K V, DENG, M. The NLRP3 inflammasome: molecular activation and regulation to therapeutics [J]. *Nat. Rev. Immunol.* **19** (8), 477–489 (2019).
- HOSS, F. & RODRIGUEZ-ALCAZAR J F, L. A. T. Z. E. Assembly and regulation of ASC specks [J]. *Cell. Mol. Life Sci.* **74** (7), 1211–1229 (2017).
- IRRERA, N. et al. The role of NLRP3 inflammasome in the pathogenesis of traumatic brain injury [J]. *Int. J. Mol. Sci.*, **21**(17). (2020).
- KIM Y K, SHIN J S, NAHM, M. H. NOD-Like receptors in infection, immunity, and diseases [J]. *Yonsei Med. J.* **57** (1), 5–14 (2016).
- MAN, S. M., KARKI, R. & KANNEGANTI, T. D. Molecular mechanisms and functions of pyroptosis, inflammatory caspases and inflammasomes in infectious diseases [J]. *Immunol. Rev.* **277** (1), 61–75 (2017).
- WEI, X. et al. Role of pyroptosis in inflammation and cancer [J]. *Cell Mol. Immunol.* **19** (9), 971–992 (2022).
- PARK, P. H. Autophagy induction: a critical event for the modulation of cell death/survival and inflammatory responses by adipokines [J]. *Arch. Pharm. Res.* **41** (11), 1062–1073 (2018).
- GHOSH, S. et al. In the eyes of the Beholder-New Mertk knockout mouse and Re-Evaluation of phagocytosis versus Anti-Inflammatory functions of MERTK [J]. *Int. J. Mol. Sci.*, **25**(10). (2024).
- DORION M F, YAQUBI, M. et al. MerTK is a mediator of alpha-synuclein fibril uptake by human microglia [J]. *Brain: J. Neurol.* **147** (2), 427–443 (2024).
- NATALICCHIO, A. et al. The myokine Irisin is released in response to saturated fatty acids and promotes pancreatic  $\beta$ -Cell survival and insulin secretion [J]. *Diabetes* **66** (11), 2849–2856 (2017).
- BOSTRÖM, P. et al. A PGC1- $\alpha$ -dependent myokine that drives brown-fat-like development of white fat and thermogenesis [J]. *Nature* **481** (7382), 463–468 (2012).
- JIANG, X. et al. Irisin protects against motor dysfunction of rats with spinal cord injury via adenosine 5'-Monophosphate (AMP)-Activated protein Kinase-Nuclear factor Kappa-B pathway [J]. *Front. Pharmacol.* **11**, 582484 (2020).
- CANIVET C, M. et al. Hepatic FNDC5 is a potential local protective factor against Non-Alcoholic fatty liver [J]. *Biochim. Et Biophys. Acta Mol. Basis Disease*. **1866** (5), 165705 (2020).
- WRANN C D, WHITE J P, SALOGIANNNIS, J. et al. Exercise induces hippocampal BDNF through a PGC-1 $\alpha$ /FNDC5 pathway [J]. *Cell Metabol.* **18** (5), 649–659 (2013).
- REZA, M. M. et al. Irisin is a pro-myogenic factor that induces skeletal muscle hypertrophy and rescues denervation-induced atrophy [J]. *Nat. Commun.* **8** (1), 1104 (2017).
- COLAIANNI, G. et al. Irisin prevents and restores bone loss and muscle atrophy in hind-limb suspended mice [J]. *Sci. Rep.* **7** (1), 2811 (2017).
- YE, X. et al. Irisin reverses insulin resistance in C2C12 cells via the p38-MAPK-PGC-1 $\alpha$  pathway [J]. *Peptides* **119**, 170120 (2019).
- LIU T Y, SHI C X, GAO, R. et al. Irisin inhibits hepatic gluconeogenesis and increases glycogen synthesis via the PI3K/Akt pathway in type 2 diabetic mice and hepatocytes [J]. *Clinical science (London, England: 2015, 129*(10): 839–50. (1979).
- MO, L. et al. Irisin is regulated by CAR in liver and is a mediator of hepatic glucose and lipid metabolism [J]. (2016). *Molecular endocrinology (Baltimore, Md)*, **30**(5): 533–542 .
- LIU, S. et al. Effects and underlying mechanisms of Irisin on the proliferation and apoptosis of pancreatic B cells [J]. *PLoS One*. **12** (4), e0175498 (2017).

31. KHELLAF, A. & KHAN D Z, H. E. L. M. Y. A. Recent advances in traumatic brain injury [J]. *J. Neurol.* **266** (11), 2878–2889 (2019).
32. GAN Z S, STEIN S C, SWANSON, R. et al. Blood biomarkers for traumatic brain injury: A quantitative assessment of diagnostic and prognostic accuracy [J]. *Front. Neurol.* **10**, 446 (2019).
33. MOON H Y, BECKE, A. et al. Running-Induced systemic cathepsin B secretion is associated with memory function [J]. *Cell Metabol.* **24** (2), 332–340 (2016).
34. TIAN D W, HU H L, SUN, Y. et al. Biological effects of eukaryotic Recombinant plasmid pReceiver-M61-BAI-1 transfection on T24 cells and HUVECs [J]. *Mol. Med. Rep.* **14** (2), 1553–1559 (2016).
35. WANG, H. & ZHANG, X. Activation of TIM1 induces colon cancer cell apoptosis via modulating Fas ligand expression [J]. *Biochem. Biophys. Res. Commun.* **473** (2), 377–381 (2016).
36. XIN, J. & SONG, X. Exploring the antiviral potential of Shikimic acid against Chikungunya virus through network pharmacology, molecular docking, and in vitro experiments [J]. *Front. Veterinary Sci.* **12**, 1524812 (2025).
37. NISHI, C. et al. MERTK tyrosine kinase receptor together with TIM4 phosphatidylserine receptor mediates distinct signal transduction pathways for efferocytosis and cell proliferation [J]. *J. Biol. Chem.* **294** (18), 7221–7230 (2019).

## Acknowledgements

None.

## Author contributions

Kuo Zhang conceived the concept and collated the methodology, as well as data collation and first draft writing and supervision. Yihui Du conducted surveys, visualizations, validations, writing reviews, and edits. Sihui Yang participated in the survey and data analysis, writing review and editing. Sunguo Zhu participated in the methodology section as well as writing review and editing. All authors read and approved the final manuscript.

## Funding

This research was supported by the S&T Program of Hebei (Grant No.22377717D), the Hebei Provincial Natural Science Foundation of China (Grant No.H2020206437), the Government-funded Provincial Medical Talent Project of China (Grant No. 303-2022-27-02) and the Key Medical Scientific Research Project of Hebei Province of China (Grant no. 20220112;20230032).

## Declarations

## Competing interests

The authors declare no competing interests.

## Ethical approval

This study has been approved by the Medical Ethics Committee of Hebei General Hospital.(Approval number: 2024-DW-011, 2024-DW-047).

## Patient consent for publication

Not Applicable.

## Additional information

**Supplementary Information** The online version contains supplementary material available at <https://doi.org/10.1038/s41598-025-00066-7>.

**Correspondence** and requests for materials should be addressed to G.S.

**Reprints and permissions information** is available at [www.nature.com/reprints](http://www.nature.com/reprints).

**Publisher's note** Springer Nature remains neutral with regard to jurisdictional claims in published maps and institutional affiliations.

**Open Access** This article is licensed under a Creative Commons Attribution-NonCommercial-NoDerivatives 4.0 International License, which permits any non-commercial use, sharing, distribution and reproduction in any medium or format, as long as you give appropriate credit to the original author(s) and the source, provide a link to the Creative Commons licence, and indicate if you modified the licensed material. You do not have permission under this licence to share adapted material derived from this article or parts of it. The images or other third party material in this article are included in the article's Creative Commons licence, unless indicated otherwise in a credit line to the material. If material is not included in the article's Creative Commons licence and your intended use is not permitted by statutory regulation or exceeds the permitted use, you will need to obtain permission directly from the copyright holder. To view a copy of this licence, visit <http://creativecommons.org/licenses/by-nc-nd/4.0/>.

© The Author(s) 2025